Theoretical Molecular Rheology of Branched Polymers in Simple and Complex Flows: The Pom-Pom Model

G. Bishko,[1] T. C. B. McLeish,[1] and O. G. Harlen[2]
[1]*IRC in Polymer Science and Technology, Department of Physics, University of Leeds, Leeds, LS2 9JT, United Kingdom*
[2]*Department of Applied Mathematics, University of Leeds, Leeds, LS2 9JT, United Kingdom*

R. G. Larson
Department of Chemical Engineering, 2300 Hayward, University of Michigan, Ann Arbor, Michigan 48109-2136
(Received 19 May 1997)

The nonlinear rheological constitutive equation of a class of multiply branched polymers is derived using the tube model. The molecular architecture may be thought of as two q-arm stars connected by a polymeric "crossbar." The dynamics lead to a novel integrodifferential equation which exhibits extreme strain hardening in extension and strain softening in shear. Calculations of flow through a contraction predict that the degree of long-chain branching controls the growth of corner vortices, in agreement with experiments on commercial branched polymers. [S0031-9007(97)04103-3]

PACS numbers: 83.10.Nn, 47.50.+d, 83.20.Fk, 83.85.Pt

Polymer melts and concentrated solutions are complex fluids whose dynamics are dominated by the topological restrictions of uncrossability of long-chain molecules. Substantial theoretical progress has been made within the framework of the tube model [1] in which the constraints on a given chain segment are modeled by a tube of diameter a, coarse graining the curvilinear path of the polymer. Two dominant modes of "entangled" dynamics at long time scales emerge: Linear polymers may change their configurations via *reptation*—or curvilinear diffusion, which leads to a sharp distribution of modes in stress relaxation and a viscosity scaling with molecular weight as $M^{3.4}$ [1–3]. Polymers with long-chain branching are constrained to *fluctuation* modes of the entangled arms, which lead to a broad relaxation spectrum and exponential dependence of viscosity on their arms' molecular weight, even in the case of simple star polymers [4,5], where the theory agrees quantitatively with experiments over a range of materials and molecular weights [6]. An additional process of *retraction* may follow large deformations by which extended chain segments with free ends rapidly regain their equilibrium contour length inside the extended tubes. This accounts for the extreme shear thinning of linear and star polymers [1]. Commercial long-chain branched polymers differ distinctly from linear polymers [7–9] in rheological response. Low density polyethylene (LDPE), in particular, which has multiple, irregularly spaced, long branches, shows "strain hardening" in transient extensional flows that differs qualitatively from the behavior of unbranched melts. In shear flow, however, the behavior of LDPE is highly "strain softening," not unlike ordinary linear polymers. Existing phenomenological constitutive theories do not capture this behavior. Even the very general integral-type equation [8], containing arbitrary functions of the strain invariants, cannot combine the observed strain hardening in both uniaxial [8] *and planar* [10] extension together with the softening in shear. Such equations therefore cannot consistently account for the special behavior which occurs in complex flows of LDPE, when implemented in non-Newtonian flow solvers [11]. In particular, linear and branched melts of identical viscosity and terminal relaxation times exhibit very different flow fields in a contraction: Linear polymers mimic Newtonian fluids, while branched polymers set up a large rotating vortex in the corner of the contraction [12,13]. A theory connecting the molecular topology to features of the flow is highly desirable. The tube model does indeed predict that the large-strain properties of branched polymers differ from the strain softening of linear polymers [14], suggesting that it might provide the missing mathematical structure if pursued to a full constitutive equation. In this Letter we show that the outcome of such a project accounts for the effects of branching in both simple and complex flows.

The class of branched polymers chosen for this study can be thought of as a generalization of the H-polymer structure [15,16]. The "pom-pom" molecules contain just two branch points of chosen functionality—a "crossbar" links two pom-poms of q arms each (see Fig. 1). Structural parameters are the molecular weight of the crossbar M_b, molecular weight of the arms M_a, and the branch number q. The entanglement molecular weight M_e [1] is another important molecular parameter, but will serve only to define the dimensionless path lengths $s_a = M_a/M_e$ and $s_b = M_b/M_e$. The model polymer contains the essential feature of a strand between the two branch points. This strand cannot diffuse at all on length scales longer than a until the relaxation of the starlike arms is complete. At longer time scales the melt may be considered as entangled crossbar strands only, diluted by the (relatively) rapidly moving arms [16] to a volume fraction ϕ_b. The crossbars therefore behave at these time scales like linear polymers with large friction at their extremities, and so diffuse by reptation. The reptation time is longer than the terminal relaxation of the arms by a factor of s_b^2, and the retraction

 0031-9007/97/79(12)/2352(4)$10.00

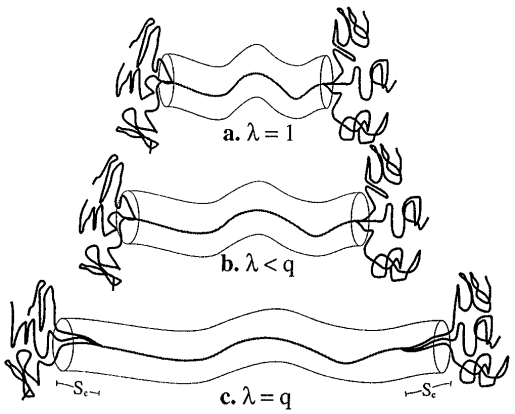

FIG. 1. The pom-pom model polymer ($q = 3$) with effective confining tube on the crossbar. Configurations are shown schematically under (a) no strain and at higher strains causing (b) no and (c) partial withdrawal of the branch points.

time by s_b, so over a wide range of deformation rates all non-Newtonian response arises from the dynamics of the crossbars alone.

The retraction of the crossbars under large strains also differs from the rapid relaxation of linear polymers and dangling arms. Instead they extend under strain until their tension is sufficient to withdraw the dangling arms into tubes originally occupied by crossbars [13]. The consequence of this new process of "branch point withdrawal" in a flow is radical: At deformation rates slow compared to the retraction dynamics of the arms yet fast enough to stretch the crossbars, some of the arm material, say s_c per arm, may be aligned with the crossbar (see Fig. 1). The frictional drag of the "blob" of the remaining relaxed arm ζ_b is then determined by the relaxation time of the now-shorter arms, which is exponentially faster in s_c:

$$\zeta_b = 2kT\frac{\tau_a(s_c)}{a^2}q\,, \tag{1}$$

where $\tau_a(s)$ is the relaxation time of the segment a distance s from the branch point. To leading order in s this varies as $\tau_a(x) = \tau_a(0)\ \exp(-15\phi_b s/4)$. The key consequence of this flow-induced renormalization of ζ_b is to limit the dimensionless stretch factor $\lambda(t)$ of the backbone to the value q determined by the degree of branching. In the limit of highly entangled backbones it becomes valid to work with preaveraged dynamic variables. The stretch then couples to the flow (with local deformation rate gradient $\mathbf{K}$) as a driven Gaussian spring [17]:

$$\frac{D}{Dt}\lambda = \lambda(\mathbf{K}:\mathbf{S}) - \frac{1}{\tau_s}(\lambda - 1)\,, \tag{2}$$

strictly for $\lambda < q$, and where $\tau_s = s_b q \tau_a(0)$ is the stretch relaxation time. D/Dt is the substantive time derivative. When the maximum stretch would be exceeded, the dynamical evolution is transferred to the variable $s_c(t)$, which measures the withdrawal and alignment [first term of Eq. (3)] of the branches:

$$\frac{Ds_c}{Dt} = \left(q\frac{s_b}{2} + s_c\right)\mathbf{K}:\mathbf{S} - \frac{1}{2\tau_a(s_c)}\,, \tag{3}$$

opposing their star-arm-like relaxation [second term in Eq. (3)]. The final dynamical variable needed to construct the stress is the second moment of the orientation distribution function $\mathbf{S}(t)$ for tube segments containing crossbars [1]. These orient in the flow, reptate, and retract, like linear polymers, but have a time-dependent reptation time (like wormlike micelles [18], but due to changes in configuration of the dangling ends rather than in molecular weight). The evolution equation for $\mathbf{S}(t)$ is therefore a simple modification of the Doi-Edwards result for entangled linear polymers:

$$\mathbf{S}(t) = \int_{-\infty}^{t}\frac{dt'}{\tau_b(t')}\,\exp\left(\int_{t'}^{t}\frac{dt''}{\tau_b(t'')}\right)\mathbf{Q}(\mathbf{E}(t,t'))\,, \tag{4}$$

where $\mathbf{Q}$ is the Doi-Edwards tensor [1] describing the average orientation at t of tube segments created at t' and deformed by $\mathbf{E}(t,t')$. The exponential term is their survival probability and the reptation time varies as $\tau_b = (4/\pi^2)s_b^2\phi_b\tau_a[s_c(t)]$. Thus we arrive at a small set of evolving structural dynamical variables $\mathbf{S}(t)$, $\lambda(t)$, and $s_c(t)$, from which the stress may be calculated. Both the tension and contour length of the crossbar increase linearly with λ, and we need to respect the quadratic scaling of modulus with volume fraction of entangled material. Extra contributions arise from arm material aligned with the crossbar. The final expression for the polymeric stress is [17]

$$\boldsymbol{\sigma} = \frac{15}{4}G_0\phi_b\left(\phi_b\lambda^2(t) + \frac{2qs_c(t)}{2qs_a + s_b}\right)\mathbf{S}(t)\,. \tag{5}$$

A "solvent stress" contribution from material relaxing at much faster rates than the flow rates (the pom-pom arms and all higher "Rouse" modes in this case) is added via a Newtonian term. In all our simulations we chose a solvent viscosity $\eta_s = G_0\tau_s/8$. Together with Eqs. (2)–(4), this defines the constitutive theory for a melt of these branched polymers at deformation rates up to $\tau_a(0)^{-1}$.

The results for extensional and shear-stress transients after the initiation of flow were computed for a system with the molecular parameters $\{q = 5,\ s_a = 3,\ s_b = 30\}$. Results are shown in Fig. 2 together with data on LDPE for comparison. The deformation rates (dimensionless in terms of the stretch relaxation time τ_s) vary from 0.045 to 6.0 (in terms of τ_b they are 6 times higher). As expected, the low rates exhibit simple stress growth to a steady-state plateau. As the extension rate is increased, a very small amount of extension thinning is observed before the crossbars begin to stretch. Throughout the range of deformation rates over which the plateau stress is growing, the equilibrium value of λ is also rising. At still higher rates, a marked change of behavior sets in: λ reaches its maximum value in finite time, and thereafter branch-point withdrawal occurs—s_c rapidly rises and finds its equilibrium value. The stress growth now shows a rapid hardening behavior which is cut off by the maximum sustainable stretch.

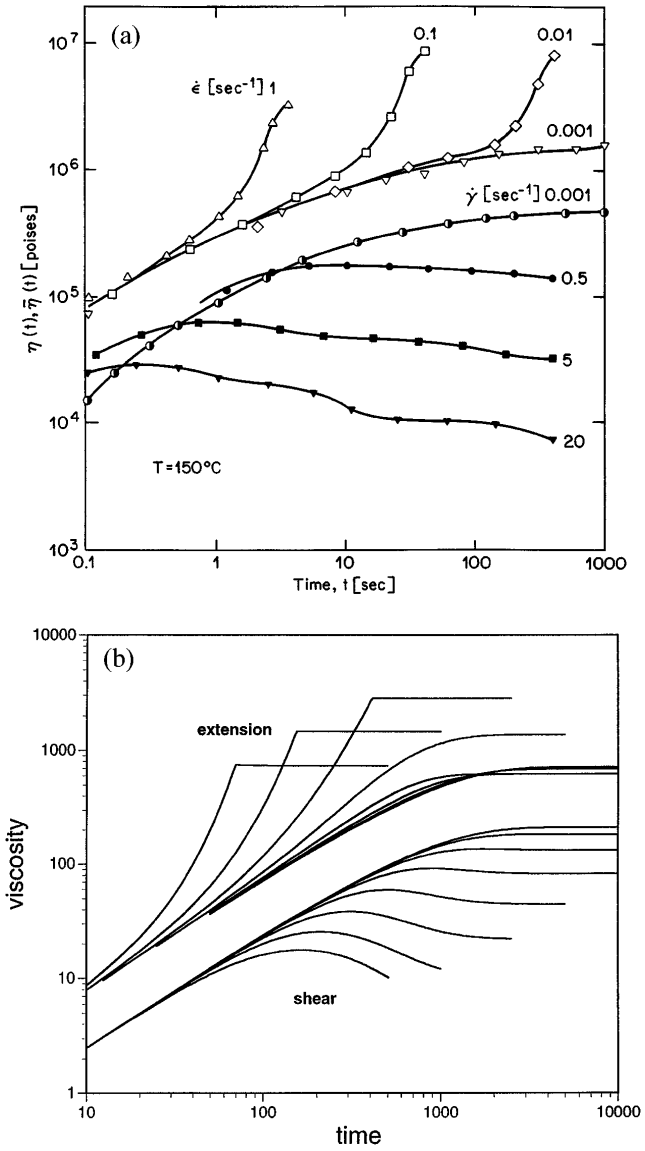

FIG. 2. (a) Start-up transient viscosities in uniaxial extension and shear for the LDPE [9]; (b) start-up viscosities for the $\{q = 5, s_a = 3, s_b = 30\}$ pom-pom model in shear and extension deformation rates are 0.045, 0.09, 0.18, 0.375, 0.75, 1.5, 3.0, and 6.0 in terms of the stretch relaxation time τ_s. Weissenberg numbers for orientation may be obtained by multiplying these rates by 6.1.

For higher deformation rates, the extension viscosity thins again as the steady-state extensional stress now grows only weakly. The qualitative similarity with extensional data on LDPE [11,19] is remarkable, and especially significant in occurring for both uniaxial *and* planar extension.

The computations for shear flow show very different behavior. Figure 2 also shows the growth of shear stress for the same range of deformation rates as before. Overshoots in the shear stress σ_{xy} are evident but lie *below* the slow-flow case. Although the backbone may stretch transiently, and even reach its maximum value, no hardening effect results in steady state, and the shear response is uniformly thinning. The unique softening behavior in shear arises because of the separation in time scale of orientation and stretch of the active crossbar segments: At rates which couple to the stretch in extension, the molecule has already aligned in shear parallel to the flow direction, reducing the coupling term $\mathbf{K}:\mathbf{S}$ in Eq. (3). This necessary separation is a direct consequence of the entangled state of the crossbar. Although LDPE is structurally more complex than the pom-pom molecule, the generic feature of a moderate separation in time scales between segmental stretch and orientation will survive. We believe this accounts for the similarities between the LDPE data and our model.

The constitutive equation set derived above retains structure of molecular significance yet is simple enough to be applied to flow in complex geometries. As an example we have chosen the "benchmark" problem of flow into a planar 4:1 contraction. The calculations were performed using a mixed Euler-Lagrange method [20] with a slightly modified version of the equations. **(**The numerical scheme utilizes a co-deforming grid of finite elements so that history-dependent quantities are local to the grid. One approximation of the equation set was necessary to make the computation feasible—the integral expression for $\mathbf{S}(t)$ was replaced by a differential approximation which has been shown to give very similar results in all flow geometries [17]: $D\mathbf{A}/Dt = \mathbf{K}\cdot\mathbf{A} + \mathbf{A}\cdot\mathbf{K}^T - \tau_b^{-1}(\mathbf{A} - \mathbf{I})$ and $\mathbf{S}(t) = \mathbf{A}(t)/\mathrm{tr}[\mathbf{A}(t)]$.**)**

Figure 3 shows the flow and molecular stretch fields $[\lambda(\boldsymbol{r})]$ of an unbranched molecule ($q = 1$) and branched pom-poms with $q = 5$. The Weissenberg number, based on the upstream wall shear rate, is unity in all cases. We $= 3Q\tau_s/2L^2$, where Q is the areal flux through the contraction and L is the upstream width of the channel. Contrasting Figs. 3(a) and 3(b), one sees that the pom-pom branching produces an enlargement of the corner vortex, a phenomenon frequently observed with branched LDPEs. From the simulation, the molecular source of this phenomenon can be discerned. The color coding shows that only the branched polymer is stretched in the contracting region by the strong extensional flow there.

Surprisingly, the maximum stretch does not occur along the center line where the extension rate is greatest, but close to the boundary between the corner vortex and the funnel of material drawn into the contraction. This can be explained by following a fluid element as it moves from the wall region into the funnel, or more simply by looking at the flow and stretch fields at earlier times. This is done in Fig. 3(c) which shows that, during the start-up transient, a high degree of stretch develops at the apex of the vortex where strand material is stripped of the wall by the sink flow. This wall material, while not stretched by the shear, is *preoriented* by it, and hence rapidly stretched by the extensional flow in the funnel. The enhanced version of this effect in the transient survives as the "wing" of high stretch in the steady flow of Fig. 3(b).

Thus, the vortex growth in a fluid with strong extension hardening arises from the need to maintain a balance between shear and extensional stresses [21]. For fluids with a high Trouton ratio, Tr (such as the pom-pom)

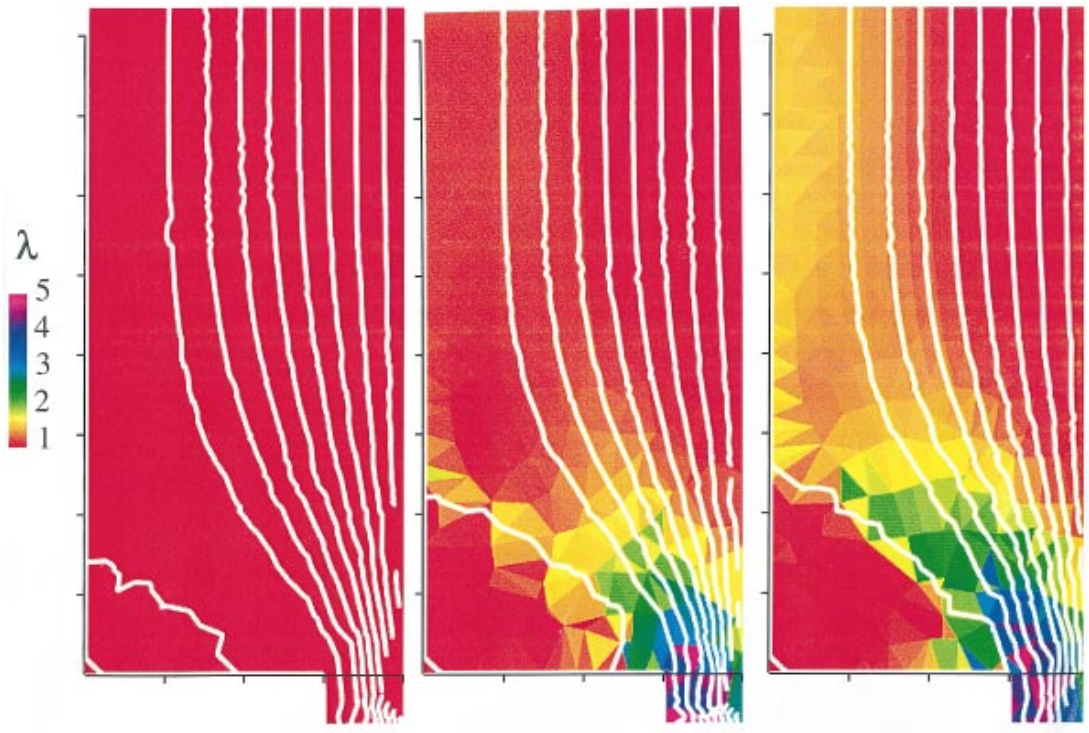

FIG. 3(color). Flow from start-up into a 4 : 1 contraction computed for the pom-pom model with fixed total and crossbar molecular. In (a) and (b) the upstream strain at the wall since initiation is 12.5. (a) We = 1, $q = 1$ (linear polymer); (b) We = 1, $q = 5$; (c) We = 1, $q = 5$ but at a transient upsteam strain of 5.0. Note the "spur" of preoriented material joining the wall and the funnel.

Keiller *et al.* showed that flow into a planar sink is confined to a narrow cone whose semiangle is proportional to $\mathrm{Tr}^{-1/2}$ [22]. Thus, higher Tr produces enlarged vortices.

The molecular modeling and simulations described here have relatively straightforward generalizations to other molecular architectures, and to polydisperse ensembles of molecules. With this new approach, molecular theory can be used to explain the influence of polymer architecture on polymeric flow fields. The progress described here may help in future designs of polymers for specific processing properties.

We thank R. C. Ball, X. F. Yuan, D. Bick, R. Keunings, and M. Wagner for useful discussions, and the Isaac Newton Institute for the Mathematical Sciences, Cambridge, for hospitality during this work. Partial funding is gratefully acknowledged from BP Chemicals and EPSRC (U.K.).

[1] M. Doi and S. F. Edwards, *The Theory of Polymer Dynamics* (Clarendon, Oxford, 1986).
[2] M. Rubinstein, E. Helfand, and D. S. Pearson, Macromolecules **20**, 822–829 (1987).
[3] M. Rubinstein, Phys. Rev. Lett. **59**, 1946–1950 (1987).
[4] D. S. Pearson and E. Helfand, Macromolecules **19**, 888 (1984).
[5] R. C. Ball and T. C. B. McLeish, Macromolecules **22**, 1911–1913 (1989).
[6] S. Milner and T. C. B. McLeish, Macromolecules **30**, 2159–2166 (1997).
[7] R. G. Larson, *Constitutive Equations for Polymer Melts and Solutions* (Butterworths, Boston, 1988).
[8] A. Kaye, College of Aeronautics, Cranford, U.K., Note No. 134, 1962; B. Bernstein, E. A. Kearsley, and L. J. Zapas, Trans. Soc. Rheol. **7**, 391 (1963).
[9] J. M. Meissner, J. Appl. Polym. Sci. **16**, 2877 (1972).
[10] T. C. B. McLeish, Phys. World **8**, 32 (1995).
[11] H. M. Laun and H. Schuch, J. Rheol. **33**, 119 (1989).
[12] R. Ahmed, R. F. Liang, and M. R. Mackley, J. Non-Newton. Fluid Mech. **59**, 129 (1995).
[13] C. D. Han and L. H. Drexler, J. Appl. Polym. Sci. **17**, 2329 (1973).
[14] D. K. Bick and T. C. B. McLeish, Phys. Rev. Lett. **76**, 2587 (1996).
[15] J. Roovers, Macromolecules **17**, 1196 (1984).
[16] T. C. B. McLeish, Macromolecules **21**, 1062–1069 (1988).
[17] T. C. B. McLeish and R. G. Larson, J. Rheol. (to be published).
[18] M. E. Cates, J. Phys. Chem. **94**, 371 (1990).
[19] H. M. Laun, in *Proceedings of the Ninth International Congress on Rheology, Acapulco, Mexico, 1984* (UNAM, Mexico City, 1984), Vol. 3, p. 535.
[20] H. K. Rasmussen and O. Hassager, J. Non-Newton. Fluid Mech. **46**, 63–99 (1993); X. F. Yuan, R. C. Ball, and S. F. Edwards, J. Non-Newton. Fluid Mech. **46**, 331–350 (1993); O. Harlen, J. M. Rallison, and P. Szabo, J. Non-Newton. Fluid Mech. **60**, 81–104 (1995).
[21] P. Szabo, J. M. Rallison, and E. J. Hinch, J. Non-Newton. Fluid Mech. (to be published).
[22] R. A. Keiller, J. M. Rallison, and J. G. Evans, J. Non-Newton. Fluid Mech. **42**, 249–266 (1992).